# An accelerated predictor-corrector scheme for 3D crack growth simulations

**W. Weber[1] and G. Kuhn[2]**

[1,2] Institute of Applied Mechanics, University of Erlangen-Nuremberg
Egerlandstraße 5, 91058 Erlangen, Germany

[1] weber@ltm.uni-erlangen.de

***ABSTRACT.*** *An accelerated predictor-corrector scheme is presented to speed up the simulation of 3D fatigue crack growth for problems with linear-elastic material behavior. Based on the highly accurate stress field - computed with the 3D dual boundary element method (Dual BEM) - the stress intensity factors (SIFs) are calculated by an extrapolation method. The crack deflection as well as the crack extension is controlled by these SIFs. Due to the nonlinear behavior of crack growth an incremental procedure has to be applied. Based on experimental evidence it is assumed that the crack front shape ensures a constant energy release rate along the whole crack front, which means a constant $K_V$. Starting from a crack front satisfying this requirement a predictor step is performed. Usually, the new determined crack front does not fulfill the requirement of a constant energy release rate. Several corrector steps are needed to find the correct crack front. Increasing the efficiency of the corrector steps, the history of the crack path is taken into account in the predictor-corrector scheme. Since the total number of simulations decreases the calculation time is reduced significantly. The efficiency of the presented predictor-corrector scheme is demonstrated by comparing numerical examples with precise experimental results.*

## INTRODUCTION

The simulation of three dimensional fatigue crack growth requires an effective numerical tool. Due to the non-linear nature of crack growth, an incremental procedure is necessary. In each loop a complete stress analysis has to be performed and the stress intensity factors (SIFs) have to be calculated. Then a 3D crack growth criterion is utilized, which controls the crack extension and the crack deflection. Finally the discretization has to be updated for the next incremental loop.

As the 3D dual boundary element method (Dual BEM) [1] is especially suited for linear-elastic stress concentration problems it is applied to solve the boundary value problem. Then, the SIFs as well as the T-stresses are evaluated at discrete points $P_i$ along the crack front by an extrapolation method. The optimized evaluation of very accurate SIFs along the crack front is done from the numerical stress field by a

regression technique controlled by the standard deviation [2]. A 3D crack growth criterion based on these SIFs determines a new crack front. It is assumed that the new crack front is characterized by a constant energy release rate along the crack front [2]. The whole concept is realized in terms of a predictor-corrector procedure.

To perform the crack growth simulation as fast as possible the complexity of the predictor-corrector concept has to be minimized. On the one hand a new predictor strategy and on the other hand an improved corrector concept are presented.

The efficiency of the optimized scheme is shown by numerical examples where both concepts are applied.

## STRESS ANALYSIS

First the boundary value problem of the current crack configuration has to be solved, cf. Fig. 1. This is done by the 3D dual boundary element method (3D Dual BEM) [1].

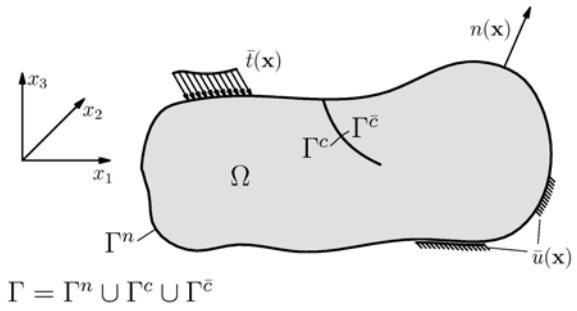


Figure 1. Sketch of the boundary value problem.

The body $\Omega \in \Re^3$ including any number of cracks is homogeneous and isotropic with linear elastic material behavior. The whole boundary $\Gamma$ of the domain $\Omega$ is divided into the normal boundary $\Gamma^n$ and the coincident crack surfaces $\Gamma^c$ and $\Gamma^{\bar{c}}$. Along the boundary $\Gamma$ Dirichlet and Neumann boundary conditions are prescribed.

Usually, it is sufficient to evaluate the displacement boundary integral equation (BIE). However, this procedure leads to a singular system matrix for problems containing a crack [3]. Hence, the coincident crack surfaces have to be separated. For this purpose the so called dual integral formulation is a suitable technique. Thus, the crack is described within one sub-region without any discretization in the area of stress concentration in front of the crack [1].

The strongly singular displacement BIE is evaluated for nodes on the normal boundary and on one crack surface. Additionally, the hyper-singular traction BIE is applied for nodes on the remaining crack surface. Both BIEs are evaluated in the framework of a collocation method.

Using the collocation method leads to a fully populated and non-symmetric system matrix. The storage capacity of this matrix is of the order $O(N^2)$ for $N$ degrees of

freedom (DOF). As long as the matrix fits into the random access memory (RAM) of the computer a fast iterative solver (GMRES) is used, which requires $O(M \times N^2)$ operations for $M$ iterations. Exceeding the memory requirements the storage capacity of the computer a slower Gaussian elimination with $O(N^3)$ operations is applied. In order to utilize the iterative solver even for such large problems the system matrix has to be compressed to fit in the RAM again.

A first attempt to reduce the memory requirements is the application of the dual discontinuity method (DDM) [4]. By introducing the discontinuities of the displacements and tractions at the crack one crack surface is eliminated for the integration. Furthermore, the linear system of equations is reduced by the DOF of one crack surface. The real displacements and tractions are calculated in a post-processing step. The DDM reduces the DOF of the set of linear equations without losing accuracy.

The effect of the DDM is valuable but less essential, if the number of DOF of one crack surface is low. To decrease the memory requirements further other matrix compression techniques have to be applied. Here, the adaptive cross matrix approximation (ACA) is utilized [5].

## AUTOMATIC 3D CRACK GROWTH ALGORITHM

The new crack front is generated in three steps as shown in Fig. 2 [6].

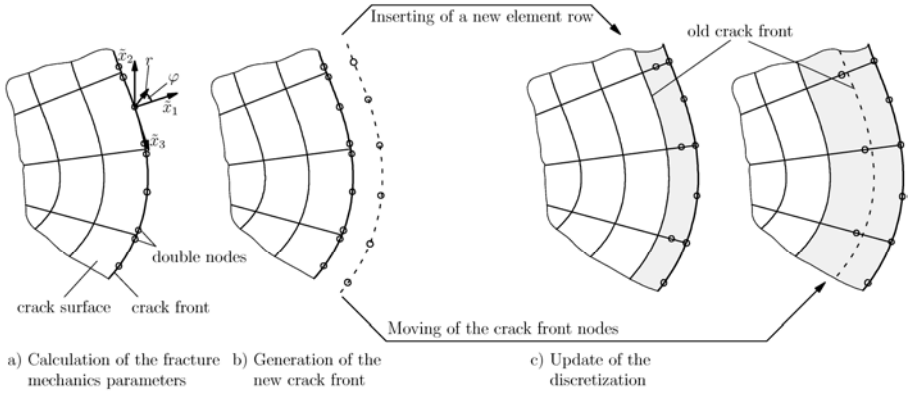


Figure 2. Three steps of an increment

First, the stress intensity factors (SIFs) have to be calculated. Therefore, discrete points $P_i$ of the 3D crack front – normally the nodes of the utilized mesh – are considered, see Fig. 2a. For each point a set of SIFs – $K_M(P)$ – and T-stresses – $T_{ij}(P)$ – are calculated from the stress near field by an extrapolation method. The results of the utilized regression analysis are optimized by the minimization of the standard deviation [2]. For points $P_i$ at a smooth crack front the typical stress distribution is given by [7]:

$$\sigma_{ij}(r,\varphi,P) = \sum_{M=I}^{III} \frac{K_M(P)}{\sqrt{2\pi r}} f_{ij}^{M}(\varphi) + T_{ij}(P) + O\left(\sqrt{r}\right). \quad (1)$$

The SIFs $K_M$ ($M = I,II,III$) characterize the intensity of the typical square root singularity while $T_{ij}$ denotes the T-stresses. $f_{ij}^{M}(\varphi)$ are the angular functions corresponding to the $M$ modes.

In the second step the new position of the crack front has to be determined by the evaluation of a suitable crack growth criterion based on the SIFs and T-stresses. The obtained crack extension as well as the kink angle define the new position of the point $P_i$, cf. Fig. 2b. The new positions of the crack front points set up the new crack front. In case of surface breaking cracks 3D corner singularities are present at the intersection of the crack front with the normal boundary [8]. Experimental observations have shown a special crack front angle $\gamma$ [9]. The angle $\gamma$ only depends on the Poisson ratio $\nu$ and the geometrical situation around the singular point. Numerical analysis of this behavior have shown that at these points the square root singularity is existent. Thereby the crack front angle can be determined by a singularity analysis for a given crack configuration and the crack extension as well as the deflection results from keeping this crack front angle.

Finally, the gap between the old and the new crack front has to be closed. Two possibilities are available. On the one hand a new row of elements is inserted [6]. This is a good choice if there are significant crack extensions for example in case of predictor steps. On the other hand in case of corrector steps only small crack extensions along the whole crack front occur. Therefore, the nodes of the old crack front are moved towards the new crack front. Surface breaking cracks require an additional treatment because the discretization of the normal surface has to be adapted. If a new row of elements is inserted a local area around the surface breaking point is re-meshed [2]. Otherwise, if only the nodes are moved, a smoothing algorithm [10] is applied. This guarantees a homogeneous mesh for reliable results in the next increment.

## OPTIMIZED PREDICTOR-CORRECTOR SCHEME

Within each increment of the 3D crack growth algorithm the position of the new crack front is determined by a crack growth criterion. Starting from the old crack front this criterion provides the crack extension as well as the crack deflection.

It is assumed that a real crack front shape ensures a constant energy release rate along the whole crack front and the direction of the crack propagation is perpendicular to the maximum principal stress. If the current crack front satisfies these requirements a new crack front is predicted. However, the determined crack front shape does usually not meet this requirements so that corrector steps are necessary. This procedure is implemented in a predictor-corrector scheme.

### Predictor

Within a predictor step the crack extension $\Delta a(P)$ and the kink angle $\varphi(P)$ for all points $P_i$ along the crack front have to be determined. The crack deflection is calculated by the maximum principal stress criterion [2].

The crack extension $\Delta a(P)$ is the more interesting part in the simulation because it differs along the crack front and it changes permanent. Therefore a user-defined incremental length $\Delta a_0$ is distributed along the crack front depending on the energy release rate $G(P)$ [11]:

$$\Delta a(P) = \Delta a_0 \frac{G(P)}{G_{max}}. \tag{2}$$

Another possibility is an exponential distribution based on the Paris-law [11]:

$$\Delta a(P) = \Delta a_0 \cdot \left( \frac{K_V(P)}{K_{V_{\max}}} \right)^m . \tag{3}$$

$m$ is the Paris-Erdogan-exponent whereas $K_V(P)$ is the effective stress intensity factor and for pure Mode I it is identical to $K_I(P)$. The requirement of a constant energy release rate is equal to a constant distribution of $K_V(P)$ along the whole crack front. This leads to a constant incremental length $\Delta a(P)$ for all points $P$. Thus, the history of the crack propagation is taken into account. Additionally to the current crack front $a_n$ the former crack front $a_{n-1}$ is considered calculating the incremental length $\Delta a(P)$. The crack extension $\Delta a(P)$ results from

$$\Delta a(P) = r \cdot \left\| x_n(P) - x_{n-1}(P) \right\|, \tag{4}$$

where $x_n(P)$ is the current position of the point $P$ and $x_{n-1}(P)$ the position at the former crack front. The factor $r$ is a relaxation parameter that controls the distance of two successive crack fronts. The relaxation factor usually ranges between 0.8 and 1.25.

This optimized prediction still needs to be controlled and if necessary the crack front shape has to be corrected. The number of corrector steps is already reduced strongly by the new concept. Further improvements can be reached by optimizing the corrector procedure.

**Corrector**

A predicted crack front usually misses the requirement of a constant energy release rate. A first approach to obtain a crack front shape meeting this requirement is the following distribution [6]

$$\Delta a(P) = \Delta a_0 \frac{G(P) - G_{min}}{G_{max}}. \tag{5}$$

Modifying the crack front with this extension leads to the desired crack front after several iterations. As every iteration is time consuming the total number of increments should be minimized. Therefore, from the second corrector step on the effect of the previous step is analyzed and the results are utilized for the present correction step by inserting a strengthening factor $s$. Furthermore, in analogy to Eq. 3 an exponential

strengthening based on the Paris-law is introduced. Thus, the incremental length is written as

$$\Delta a(P) = s\,\Delta a_0 \left[ \left( \frac{G(P)}{G_{\min}} \right)^{\frac{m}{2}} - 1 \right]. \tag{6}$$

The exponent $m$ denotes the Paris-Erdogan-exponent as shown in Eq. 3. The strengthening factor $s$ is calculated by analyzing the reduction of the variation of $K_V$.

$$s = \left( \frac{1}{n} \sum_{i=1}^{n} \frac{K_V^a(P_i) - \overline{K}_V}{K_V^o(P_i) - K_V^a(P_i)} \right)^{\frac{1}{m}} \tag{7}$$

In this equation $K_V^a(P_i)$ is the actual effective stress intensity factor at the $i$-th point out of $n$ analyzing points along the crack front. $K_V^o(P_i)$ is the effective stress intensity factor of the previous crack front and $\overline{K}_V$ is the averaged effective stress intensity factor of the current crack front.

## NUMERICAL EXAMPLE

The efficiency of the presented predictor-corrector scheme is demonstrated by a fatigue crack growth experiment. This scheme can also be applied to mixed-mode problems but already mode-I problems raise many interesting questions. Furthermore, many failures in industrial applications are caused by mode I and for this mode well documented experimental results are available. Fig. 3 shows the considered 4-point bending specimen with an "M"-shaped cross section.

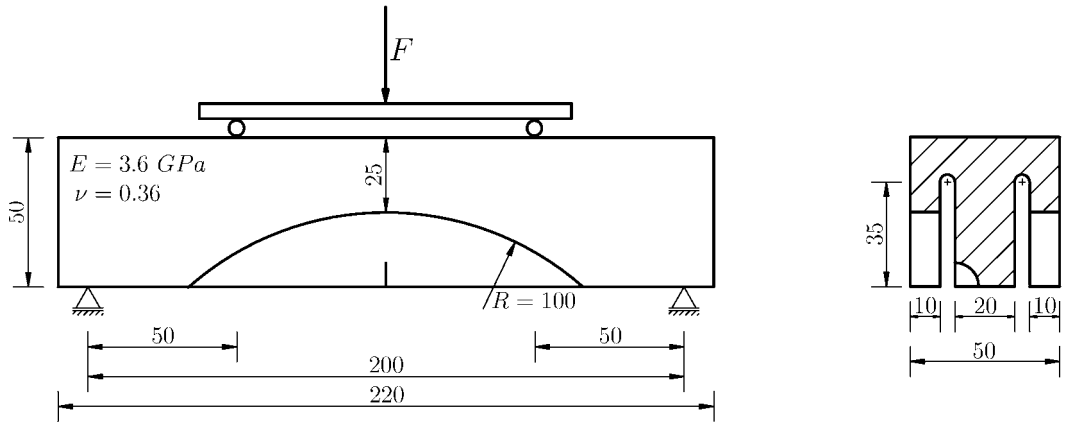


Figure 3. Four point bending specimen

In the middle of the center leg a quasi-elliptical corner crack is located. To be able to observe the crack growth the transparent material PMMA (E ≈ 3.6 GPa, ν ≈ 0.36) is

used. The force $F$ of the cyclic loads was reduced from $F = 3$ kN down to $F = 1.6$ kN to guarantee stable crack growth conditions during the whole crack propagation.

The experimental results [12] are shown in Fig. 4. First, the crack grows in both directions – horizontal and vertical – at approximately the same speed. The closer the crack approaches the rear surface the faster the crack grows horizontally compared to vertically. When the crack reaches the rear surface it grows rapidly in this region whereas on the front side crack arrest is observed. Afterwards, stable crack growth along the whole crack front is monitored once again.

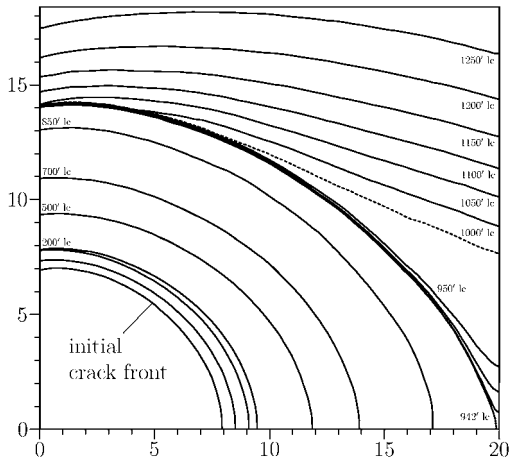


Figure 4. Experimental crack front shapes [12]

The numerical simulations, as shown in Fig. 5, start with the situation after 200.000 load cycles. In Fig. 5a the simulation with the conventional predictor-corrector scheme is shown whereas in Fig. 5b the simulation with the optimized predictor-corrector scheme is presented. The first predictor step is identical in both cases. The application of the new corrector scheme leads to a reduced number of corrector steps by one-third. Using the new predictor length, the next four predicted crack front shapes only require up to three corrector steps while with the classical concept obviously more steps are needed.

Another interesting part in this simulation is the behavior of the predictor-corrector scheme after reaching the rear surface. Using the new scheme, the number of corrector steps is reduced from more than 60 steps down to 16 steps to obtain a crack front shape with a constant energy release rate.

Overall, a broad reduction of the corrector steps (factor > 3) is observed by applying the new predictor-corrector scheme.

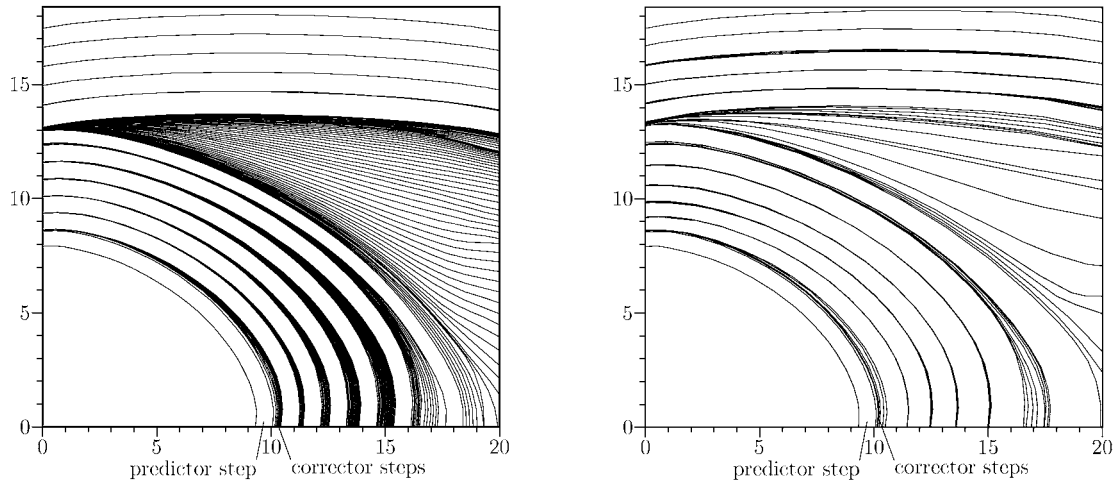


a) conventional predictor-corrector scheme b) optimized predictor-corrector scheme

Figure 5. Numerical simulation of the crack growth

## REFERENCES


1. Portella, A., Aliabadi, M.H., Rooke, D.P. (1992) In: *International Journal for Numerical Methods in Engineering* **33**, pp.1269-1287
2. Kolk, K. (2005) *Automatische 3D-Rissfortschrittssimulation unter Berücksichtigung von 3D-Effekten und Anwendung schneller Randelementformulierungen*, VDI-Verlag, Düsseldorf
3. Cruse, T. A. (1972) In: *The Surface Crack: Physical Problems and Computational Solutions*, pp.153-170, Swedlow, J. L. (Ed.), ASME
4. Partheymüller, P., Haas, M., Kuhn, G. (2000) In: *Engineering Analysis with Boundary Elements* **24**, pp.777-788, Elsevier, Netherlands
5. Kolk, K., Weber, W., Kuhn, G. (2005) In: *Computational Mechanics* **37**, pp.32–40, Wriggers, P., (Ed), Springer-Verlag, Berlin
6. Kolk, K., Kuhn, G. (2005) In: *Fatigue and Fracture of Engineering Materials and Structures* **28**, pp.117-126, Blackwell Publishing Ltd.
7. Leblond, J., Torlai, O. (1992) In: *International Journal of Elasticity* **29**, pp.97-131
8. Dimitrov, A., Andrä, H., Schnack, E. (2001) In: *International Journal of Numerical Methods in Engineering* **52**, pp.805-827
9. Heyder, M., Kolk, K., Kuhn, G. (2005) *Engineering Fracture Mechanics* **72**, pp.2095–2105, Elsevier, Netherlands
10. Blacker, T.D. (1991) In: *International Journal of Numerical Methods in Engineering* **32**, pp.811-847
11. Partheymüller, P. (1999) *Numerische Simulation der 3D-Rissausbreitung mit der Randelementmethode*, VDI-Verlag, Düsseldorf
12. Heyder, M. (2006) *Experimentelle und numerische Untersuchung der dreidimensionalen Ermüdungsrissausbreitung*, ibidem-Verlag, Stuttgart